10 Radio-frequency (RF) system

A. Andersson, D. Einfeld, F. Perez, and A. Salom

10.1 Introduction

In an electron storage ring the electrons lose energy from emitting synchrotron radiation when they are deflected in a magnetic field of the bending magnet or of the insertion devices. One of the functions of the RF system is to restore this lost energy. Therefore, an RF system with enough power to achieve this purpose must be provided. In addition, the RF system plays the role of providing stability to the beam and a large energy acceptance in order to achieve a long lifetime. As the length of the electron bunch depends on the characteristics of the RF voltage, one finds that the pulse length and the repetition rate of the emitted synchrotron radiation also depend on the RF frequency.

The transfer of power to the electrons is done by a high-frequency electromagnetic field inside the cavities. At the SEE-LS, powers between 200 and 400 kW have to be transferred to the cavities. The high-frequency electromagnetic field is generated in the amplifiers and transferred to the cavities through the waveguide system. A picture of the RF system of the synchrotron light source ANKA, where one klystron feeds two cavities, is shown in Fig. 10.1. A schematic overview of the whole RF system is given in Fig. 10.2.

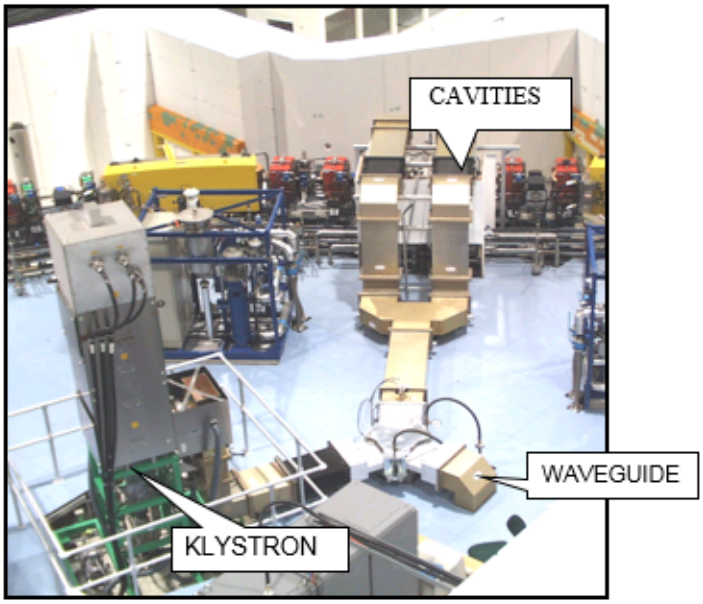

Fig. 10.1: RF system of the ANKA storage ring. A 250 kW microwave power is produced in the klystron. The power passes a circulator, which protects the klystron from the reflected power, is split into two arms by a Magic T, and is then transferred into two cavities.

https://doi.org/10.23731/CYRM-2020-001.89

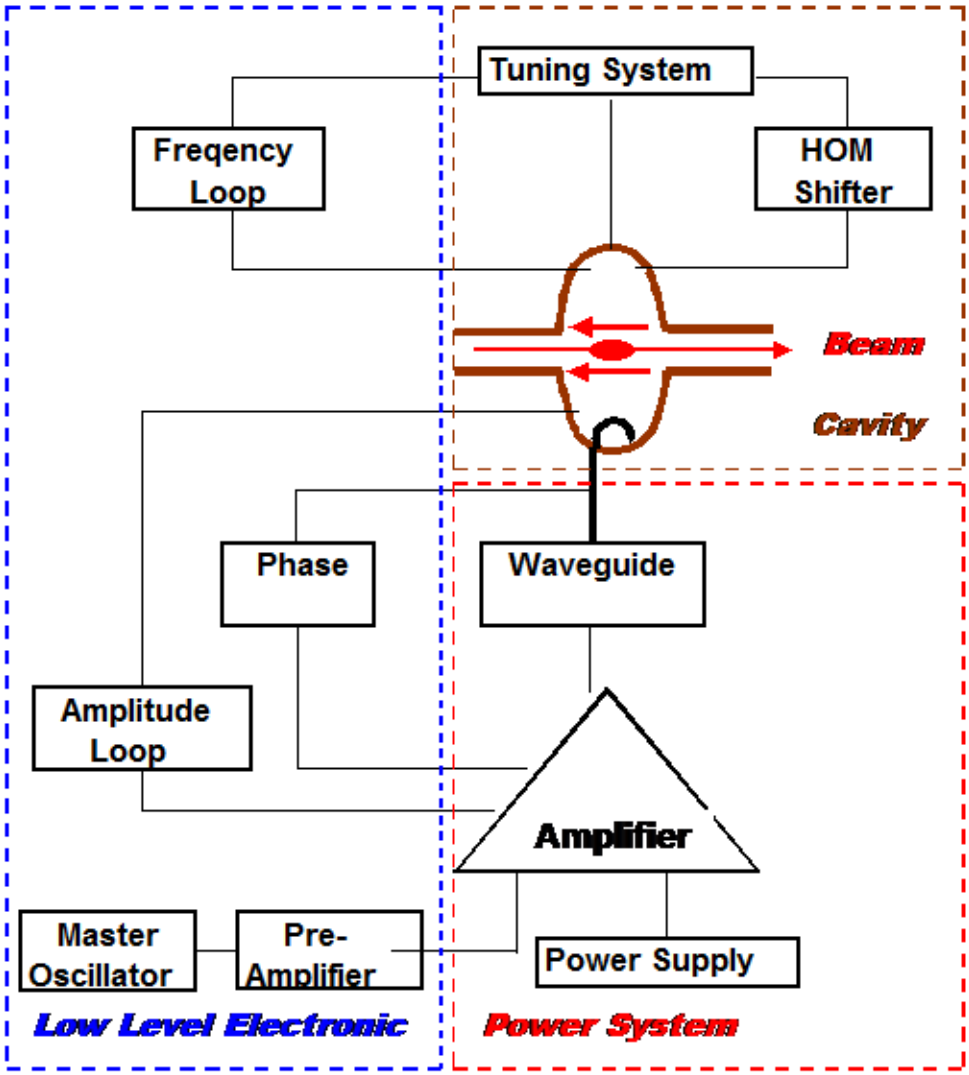

Fig. 10.2: Schematic layout of the RF system for a synchrotron light source; the main groups in the system are the cavities, the power system, and the low-level electronics.

10.2 Components of the RF system

10.2.1 Cavities

A cavity is a resonant structure, a metallic empty volume. Inside it, an electromagnetic field resonates at certain frequencies that are determined by the geometry of the structure. Cavities have a cylindrical geometry, are made of high-conductivity copper, and have some holes to allow the electrons to enter and exit the cavities on their way around the accelerator, the RF power to be fed into the cavity, and pick-up coils for diagnostics and a vacuum pump to be installed.

One of the cavities of MAX IV is shown in Fig. 10.3.

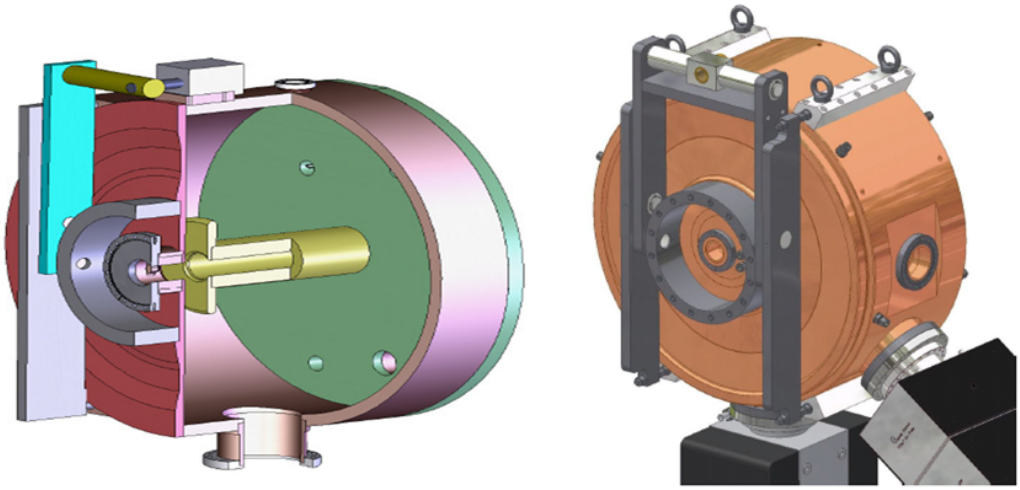

Fig. 10.3: A 3D view of the 100 MHz MAX IV cavity; the length of the cavity is 376 mm and the diameter is 920 mm.

The fundamental mode of the cavity has a frequency of 99.931 MHz, to reach a wavelength of exactly 3.0 metres. The characteristics of the cavity are given by the shunt impedance R_S and the quality factor Q (see Table 10.1). The acceleration of the beam occurs with the fundamental mode.

Furthermore, the cavities have higher-order modes that also react with the beam and lead to so-called multi-bunch instabilities. A well-established method for dealing with multi-bunch instabilities is fine-tuning of the high-order modes of the cavities by accurate mechanical movement of the endplate.

Table 10.1: Fundamental mode parameters

Parameter	Unit	Value
Frequency	MHz	99931
Quality factor, Q		19200
Shunt impedance, Rs	MΩ	0.8
Max. cavity voltage	kV	300
Max. cavity power	kW	56
Max. coupler power	kW	112

10.2.2 Amplifier

A klystron is a high-power RF amplifier with an amplification factor of about 10 000 (a gain of 40 dB). It is driven by a 25 W solid state amplifier that in turn has to be driven by a signal generator, which creates the 500 MHz primary signal.

10.2.3 Waveguide system

The waveguide system connects the amplifier to the cavities and is the path for the RF power. The power out of the amplifier passes a circulator, which is a three-port waveguide system that isolates the amplifier from the cavities. Any reflected power from the cavities is dumped into a water load installed in one of the ports. The power is then split into two by a Magic T (evenly in amplitude and in phase) and transferred to the two cavities.

Bi-directional couplers are used to monitor forward and reflected power in the line. There are four: one after the amplifier, one after the circulator, and two before the two cavities. A phase shifter in one arm going to one cavity adjusts the phase between the two cavities.

Two water loads, one in the third arm of the circulator and the other in the fourth arm of the Magic T, dissipate any reflected power. Transitions, bends, and straight sections complete the line. All the components will be able to cope with the full power, 250 kW.

10.2.4 Low-level electronics

Each of the RF units has to be controlled by a complete low-level system with which to adjust the frequency, amplitude, and phase of the RF signal in the cavity. This is achieved with the so-called tuning, amplitude, and phase loops (see Fig. 10.2).

With the frequency loop, the cavity is maintained in resonance with respect to the master oscillator frequency. In practice it is set slightly out of resonance to obtain greater stability. An amplitude loop for each RF plant is used to maintain the voltage in the cavities at the required value. The phase loop is used to keep the phase between the plants constant.

10.2.5 Principle of operation

The cavity is connected over the waveguide system with the RF amplifier, which feeds the high-frequency power P_{gen} from the amplifier into the cavity (see Fig. 10.4). This RF power builds up an electric field, which accelerates the beam. The electron bunch within the cavity has a fixed relationship to the electric field, given by the synchronous phase Φ(0). At the phase Φ(0) the electron is on average getting back the energy losses according to the emission of synchrotron light.

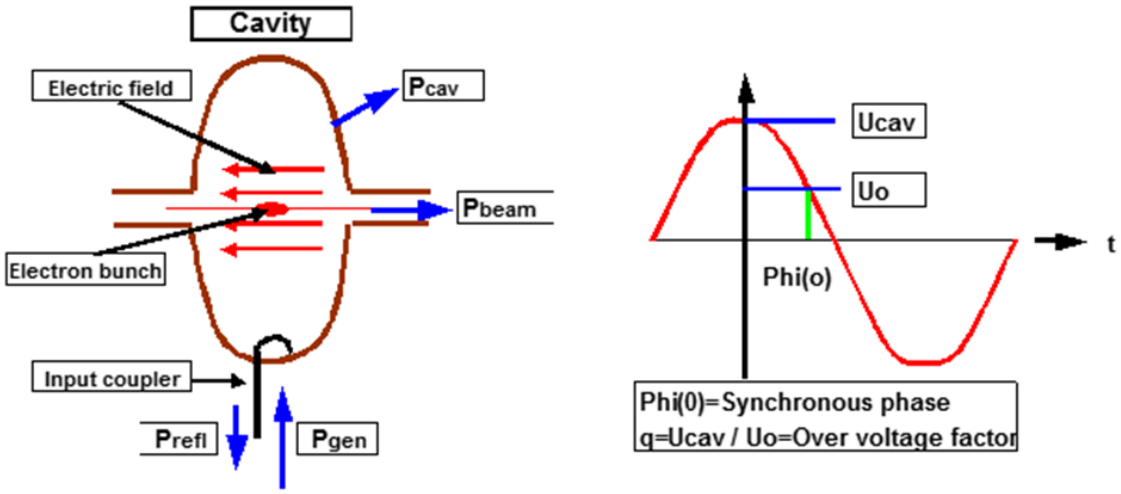

Fig. 10.4: Schematic illustrations of the expressions used in the RF system

The phase Φ(0) has to be at the falling slope of the electromagnetic field, as shown in Fig. 10.4. The circumference of the accelerator must be an integer multiple of the wavelength of the RF system. For the SEE-LS the intention is to use a 100 MHz system with a wavelength of exactly 3.0 m. The integer is called the harmonic number.

According to the conservation of power, the power of the generator is the sum of the beam, cavity, and reflected power:

$$P_{\text{gen}} = P_{\text{cav}} + P_{\text{beam}} + P_{\text{refl}} \ , \tag{10.1}$$

$$P_{\text{cav}} = U_{\text{cav}}^2 / (2R_{\text{S}}) \ , \tag{10.2}$$

$$P_{\text{beam}} = I \cdot U_0 \ . \tag{10.3}$$

Here R_s is the shunt impedance of the cavity, I is the current of the stored electrons in the accelerator, and U_o represents the energy losses to synchrotron radiation by travelling through the bending magnets, wigglers, and undulators or other insertion devices. These losses are given in Eqs. (10.4) and (10.5):

$$U_{0,\mathrm{bend}} = 88.5\,\mathrm{keV}\cdot\left(E[\mathrm{GeV}]\right)^4 / \rho[\mathrm{m}]\ , \tag{10.4}$$

$$U_{0,\mathrm{wigg}} = 0.633\,\mathrm{keV}\cdot L[\mathrm{m}]\cdot\left(E[\mathrm{GeV}]\right)^2\cdot\left(B_{\mathrm{m}}[\mathrm{T}]\right)^2\ . \tag{10.5}$$

where:

E is the energy of the electrons;

ρ is the deflection radius in the bending magnets;

B_{m} is the peak field;

L is the length of insertion device.

The reflected power is zero if the coupling factor of the input coupler has a value of

$$\beta_{\mathrm{opt}} = 1 + (P_{\mathrm{beam}} / P_{\mathrm{cav}})\ . \tag{10.6}$$

Due to the fact that more than one cavity will be installed in such a machine, it is necessary to adjust the phase of the microwave inside each cavity so that all of them act coherently to accelerate the beam. The phase between the cavities is determined by the path length of the electron orbit between them, taking into account the fact that the velocity of the electrons is the velocity of light.

10.3 RF system parameters

The parameters of the stored beam—such as bunch length, synchrotron frequency, and energy acceptance—are functions of the main parameters of the storage ring, which are summarized in Table 10.2.

The parameters of the RF system are determined by the power loss according to the synchrotron radiation and the required lifetime of the beam. With an average pressure of 2 nTorr and an energy acceptance of 4%, the so-called gas lifetime and Touschek lifetime are within the same order of magnitude, 6–8 hours. The Touschek lifetime is affected by the energy acceptance of the machine, which is determined by the energy acceptance $\varepsilon_{\mathrm{HF}}$ and the bunch length σ_l of the stored electron beam. For example, by increasing the energy acceptance from 3% to 6%, the lifetime would increase by a factor of 2; this means that the overvoltage factor must be as high as possible. Both factors, as well as the synchrotron frequency and the longitudinal tune value, are determined by the overvoltage factor q. The dependence relations are given in Eqs. (10.7)–(10.13) and in Figs. 10.5 and 10.6:

$$U_0 = V_{\mathrm{cav}}\sin(\Phi_{\mathrm{S}}) = \frac{1}{q}V_{\mathrm{cav}}\ , \tag{10.7}$$

$$\varepsilon_{\mathrm{rf}} = \sqrt{k_1\cdot F(q)}\ , \tag{10.8}$$

$$k_1 = \frac{U_0}{\pi\alpha h E_0}\ , \tag{10.9}$$

$$F(q) = 2\left\lfloor\sqrt{q^2-1} - \arccos(1/q)\right\rfloor\ , \tag{10.10}$$

$$k_2 = \frac{\alpha h}{\sqrt{2}}\cdot\sqrt{k_1}\ , \tag{10.11}$$

$$\nu_S = k_2 \sqrt{q \cos(\Phi_S)} \ , \tag{10.12}$$

$$\sigma_l = \frac{\alpha \sigma_E C}{2\pi} \cdot \frac{1}{\nu_S} \ . \tag{10.13}$$

where:

U_0 is the energy loss per turn;

Φ_s is the synchronous phase;

q is the overvoltage factor;

α is the momentum compaction factor;

h is the harmonic number;

σ_E is the relative energy spread of the beam;

ν_s is the longitudinal tune value;

C is the circumference of the machine.

Table 10.2: RF main parameters for the SEE-SL (r.m.s. is the root mean square value)

Parameter	Symbol	Value	Unit
Energy	E	2.50	GeV
Current	I_0	400.00	mA
Circumference	C	348.00	m
Momentum compaction	α	2.880E-04	
Energy loss per turn	U_0	0.233	MeV
RF frequency	F_{rf}	100.00	MHz
RF harmonic number	h	116	
Peak effective RF voltage	V_{rf}	1.40	MV
Overvoltage factor	q	6.00	
Bucket size	ε_{max}/E	0.090	
Synchrotron phase angle	Φ_S	9.60	degree
Synchrotron frequency	Ω_S	9.28	kHz
Natural r.m.s. energy spread	$\sigma E/E$	7.14E-04	
Bunch current in multi-bunch mode	I_b	3.45	mA
R.m.s. bunch length at zero current	σ_{S0}	6.65	mm
R.m.s. bunch length at zero current	σ_{S0}	22.17	psec
Peak current in multi-bunch mode		72.04	A
Vacuum chamber half-height	b	8.00	mm
Vacuum chamber half-width	h	11.00	mm
Vacuum chamber cut-off frequency	$\omega c = c/b$	37.47	GHz

10.4 RF system for the SEE-LS

The new generation of synchrotron light sources, of which MAX IV was the first to be realized, is based on a new type of lattice, the so-called multi-bend achromats, where the dispersion function is not allowed to grow to large values. From this principle it follows that the light sources can limit the

horizontal emittance to values lower than a tenth of the conventional ones. However, it follows also that the linear lattice momentum acceptance (determined by the chamber aperture and dispersion function) can be two to three times larger than before and reach values above 5%. Thus, the RF momentum acceptance, or bucket height, should be adapted to this new situation. An RF system of low frequency has an advantage in this respect. Even for a relatively low overvoltage, the ratio of total cavity voltage over energy loss per turn, one can easily reach a bucket height exceeding 5%. An overvoltage of less than 2 will be sufficient for this, and the RF system costs can be kept relatively low. A low-frequency RF system also brings the advantage of a beam spectrum that is limited to relatively low frequencies, because of the longer bunches. This property both limits the RF heating of vacuum chamber components and makes it easier to combat several kinds of high charge instability, in particular coupled-bunch instabilities driven by higher-order modes in the cavities and transverse coupled-bunch instabilities driven by the resistive walls of the compact vacuum chambers. A third advantage is that one may look at the possible bunch lengthening with higher harmonic cavities (HHCs). For example, a bunch lengthening of a factor of 5 is well within reach for a 100 MHz system, whereas for a 500 MHz system this would require so-called overstretching of the bunches. The bunch lengthening by the HHC is crucial for keeping the dilution of the transverse emittances from intra-beam scattering to reasonable levels.

10.5 RF system configuration

The local lattice momentum acceptance for the proposed ring lattice will end at around 6%, even in parts where the dispersion is at a maximum. It is therefore reasonable to aim for 6% RF momentum acceptance. The radiation losses per turn for the bare lattice are 233 keV/turn, and a reasonable assumption is that they could increase to 800 keV/turn for a ring with 15 insertion devices.

For a 100 MHz system with a total RF voltage of 1500 kV, i.e. an overvoltage of 1.875, the bucket height would end at 6%. By choosing the cavity solutions from MAX IV [10.1], one would end up with an RF configuration as in Table 10.3. There we have used the actual measured Q-values for the MAX IV cavities, which deviate slightly from the (conservatively) estimated ones in Ref. [10.1]. A plausible configuration at the commissioning stage is also presented. The same bucket height is reached but at considerably lower RF voltage. A lower RF voltage per cavity is recommended during commissioning, while the vacuum conditions are worse and the field intensity at which sparking becomes an issue (the Kilpatrik limit) is lower.

It is interesting to see that for the final phase, five RF cavities would do the job, and a transmitter size of 100 kW for each cavity would suffice. This would give a good safety margin compared to the MAX IV case, especially regarding the maximum power rating for power couplers and for circulators. The RF configurations for phase 1 and phase 2 are presented in Table 10.3. Phase 1 is for the commissioning and first operation of the system, with four insertion devices and an overall energy loss of 80 keV; phase 2 is the final phase, with the installation of 12 insertion devices and an overall loss of 240 keV.

The flange-to-flange distance for the main cavities is 0.50 m, while it is slightly longer for the Landau cavities. In the present lattice there are two short straight sections of 0.77 m placed symmetrically in the achromat. The second of these short straight sections could possibly house one cavity (the first straight section cannot be used for cavities since the ID light would have to pass here). In this way, no long straight section needs to be sacrificed for RF, but all 15 can be used for IDs. An example of such an installation is shown in Fig. 10.6. The main and Landau cavity (LC) inner profiles are shown in Figs. 10.5 and 10.7, respectively.

Table 10.3: RF configuration for the 2.5 GeV ring

Parameter	Phase 1	Phase 2
Energy loss	310 keV	500 keV
Current	200 mA	400 mA
Total SR power	62 kW	200 kW

Main RF configuration for 6% bucket height		
Total RF voltage	0.9 MV	1.5 MV
Number of cavities	3	5
Cavity voltage	300 kV	300 kV
Cavity R_{sh} ($= V^2/(2P)$)	0.8 MΩ	0.8 MΩ
Cu losses per cavity	56 kW	56 kW
Optim. coupl. (beta)	1.3	1.7
No. of RF stations	3	5
Minimum RF station power (with LC losses)	77 kW	96 kW
Landau cavity configuration		
Total LC voltage	257 kV	412 kV
Number of LCs	2	2
LC R_{sh} ($= V^2/P$)	5.3 MΩ	5.3 MΩ
Total LC Cu losses	6.2 kW	16 kW

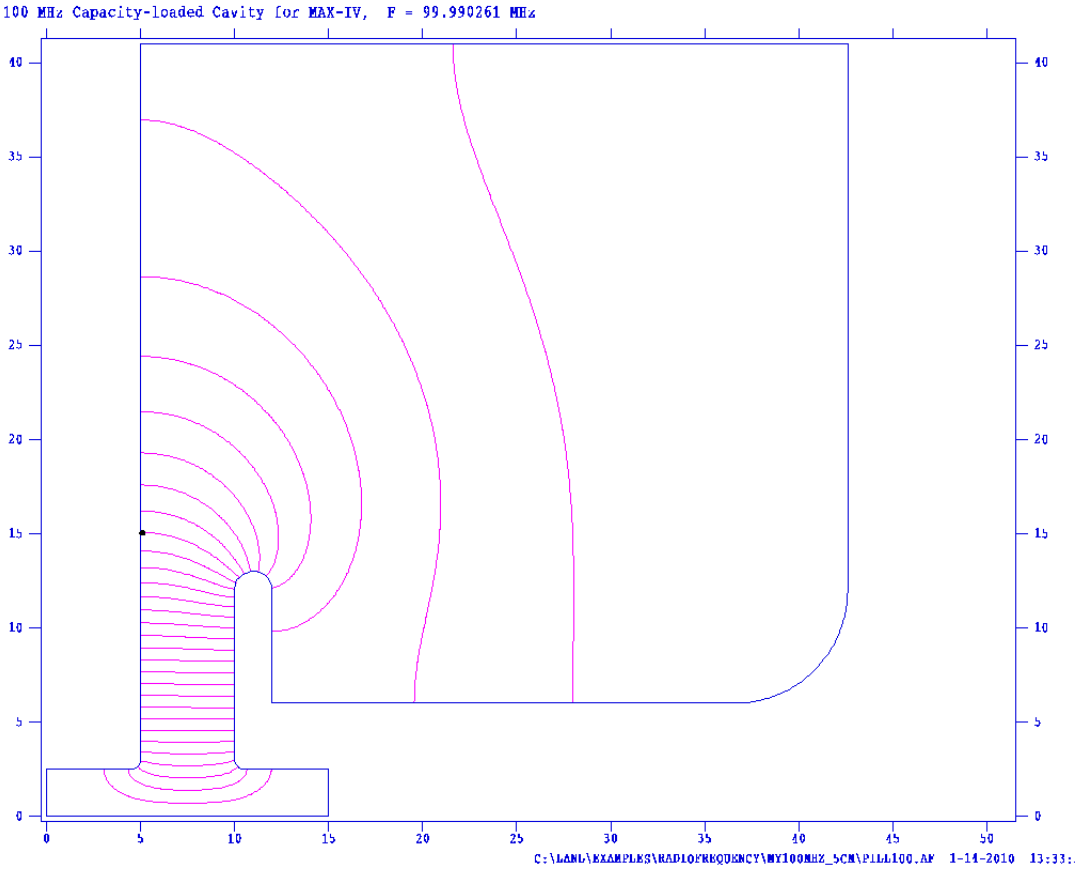

Fig. 10.5: Main cavity inner profile, where the horizontal axis is the beam axis and the vertical axis represents any radial direction; units are centimetres. The length of the cavity is 376 mm and the diameter is 920 mm.

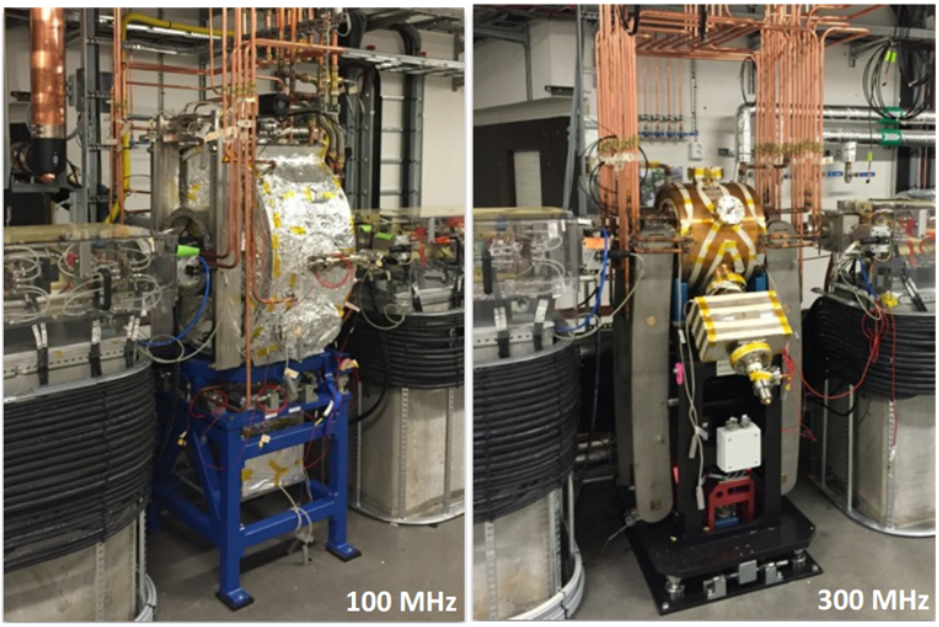

Fig. 10.6: A main cavity and the Landau cavity as installed in the MAX IV 3 GeV ring

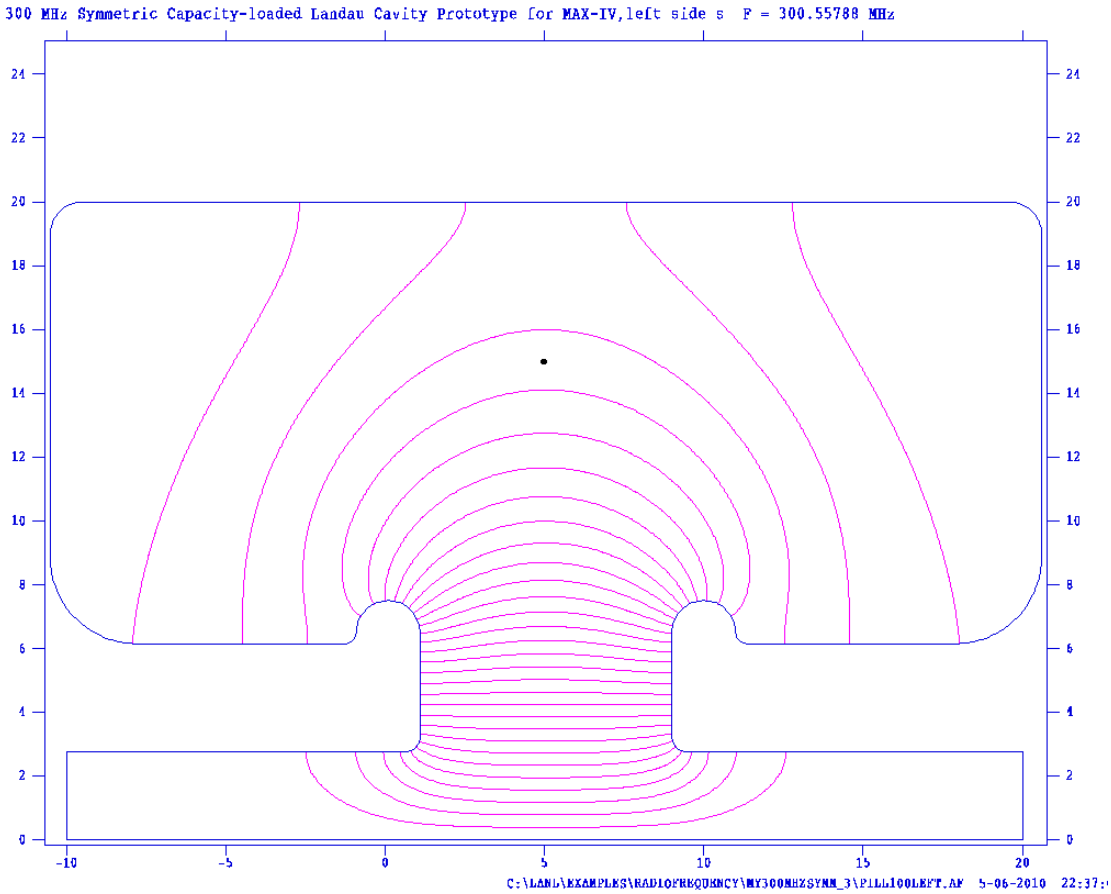

Fig. 10.7: Landau cavity inner profile, where the horizontal axis is the beam axis and the vertical axis represents any radial direction; units are centimetres.

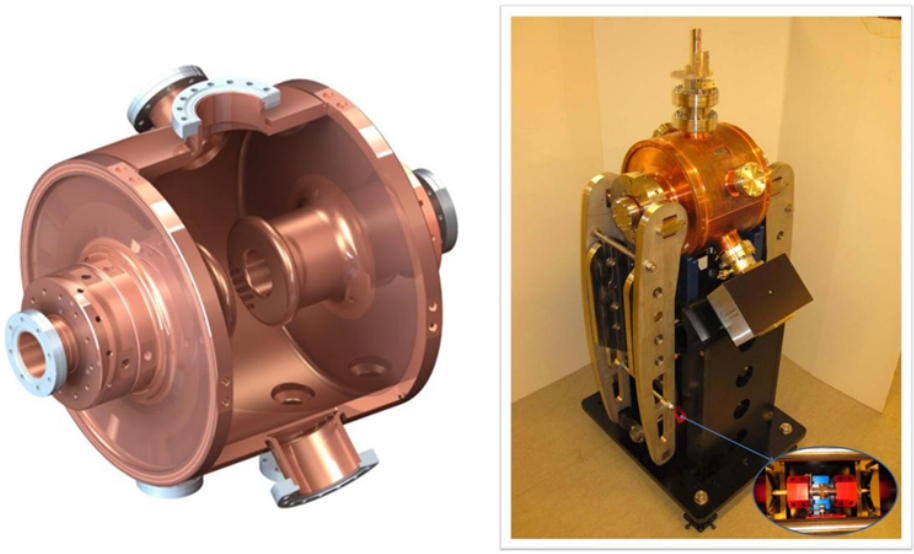

Fig. 10.8: A 3D view of the Landau cavity (left-hand side) and the support of the Landau cavity (right-hand side) as used for the installation in the ring.

Table 10.4: Beam RF parameters for 2.5 GeV ring (r.m.s. is the root mean square value)

Parameter	Phase 1	Phase 2
Synchrotron frequency without LC	1.107 kHz	1.416 kHz
Synchrotron phase without LC	163°	148°
Main cavity detuning (Q = 19700)	−6 kHz	−9.5 kHz
LC detuning (Q = 20800)	56 kHz	71 kHz
Bunch r.m.s. length without LC (at σ_E = 0.07143%)	9 mm	7 mm
Bunch r.m.s. length without LC (at σ_E = 0.07143%)	50 mm	42 mm
Peak current	3.9 A	11.5 A

From Table 10.4 we can see that with a fully ID-equipped ring, at the final phase bunch lengthening by a factor of six can be expected, which would bring the peak bunch current down from 69 A to 11.5 A. In reality the bunch shape will deviate from the quartic flat-potential shape, and a slight further elongation, of up to 44 mm, can be achieved by detuning one Landau cavity away from 3 × RF while tuning the other towards the 3 × RF line. However, the total power dissipated in the Landau cavities will increase, so the benefit will probably be quite limited. This kind of choice is the same as has been argued in Ref. [10.2], where it is shown that installing a higher Landau cavity shunt impedance than necessary for the exact flat-potential case may be beneficial in combating the Robinson instability. Figure 10.9 shows the bunch shape at the commissioning phase and Fig. 10.10 the shape at the final phase. The lower curve in each figure should be disregarded. Figure 10.11 shows the ideal quartic shape that results from a perfect matching of the product current × total Landau cavity shunt impedance.

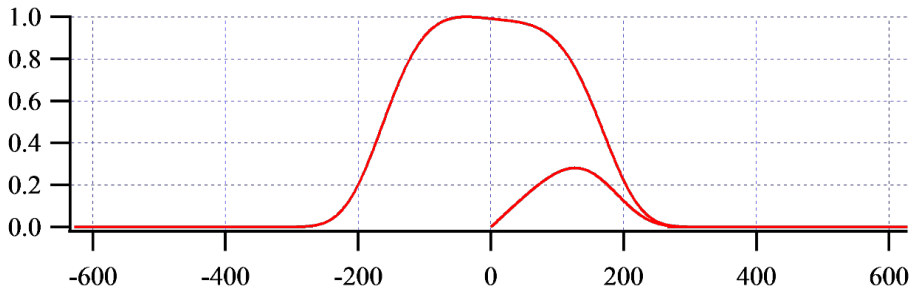

Fig. 10.9: Bunch shape at the anticipated ‘commissioning phase’; horizontal axis is in mrad RF phase

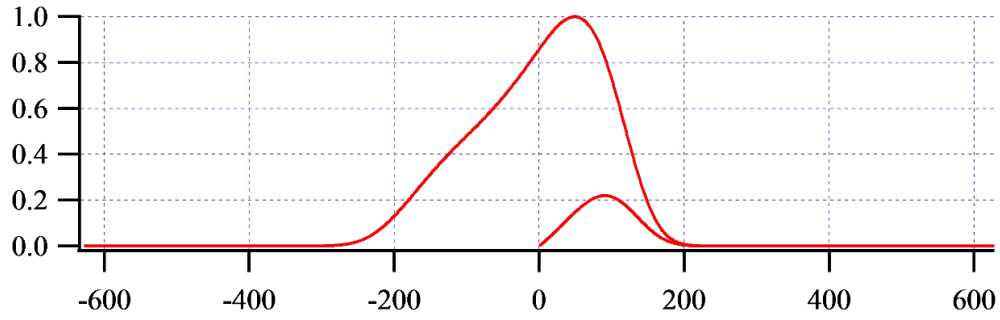

Fig. 10.10: Bunch shape at the anticipated 'final phase'; horizontal axis is in mrad RF phase

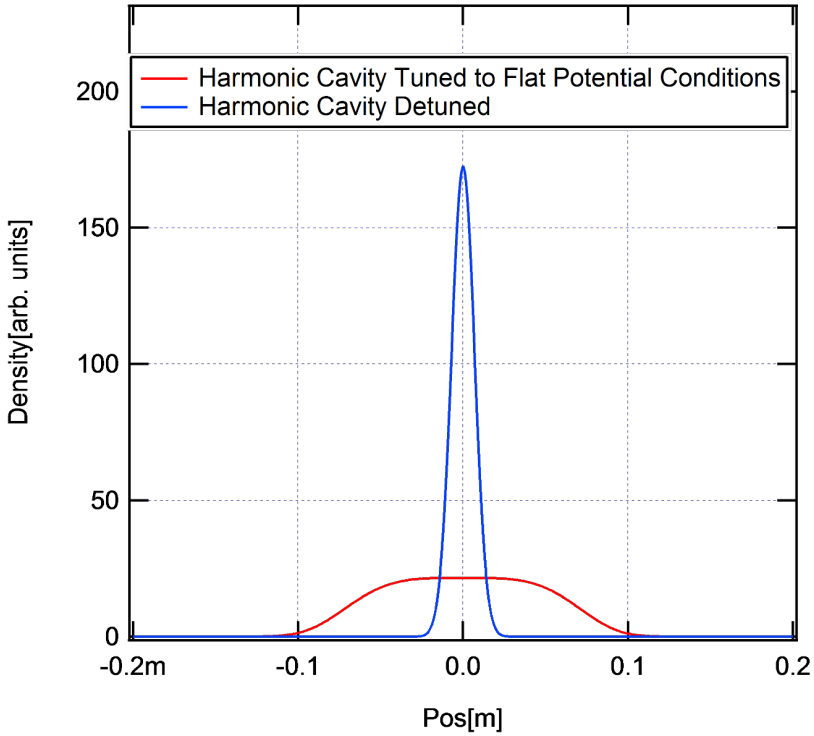

Fig. 10.11: Bunch shape without harmonic cavities (blue) and with harmonic cavities tuned to the 'flat-potential' for the fully ID-equipped ring parameters (red).

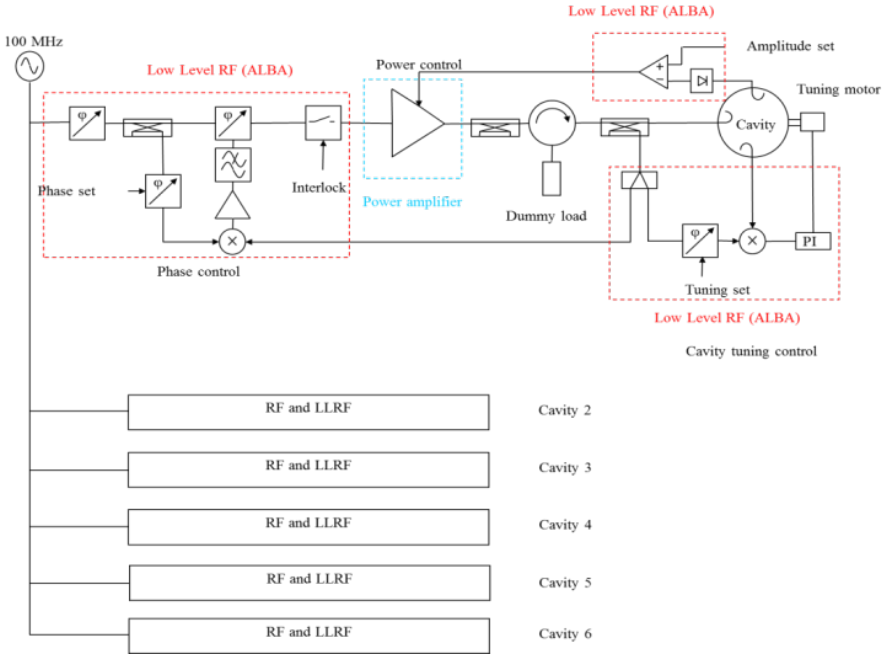

Fig. 10.12: Block diagram of the 2.5 GeV RF system

10.6 Digital low-level RF system

10.6.1 Introduction

The proposed digital low-level RF (LLRF) system should be capable of controlling the amplitude and phase of the RF voltage of the cavities at 100 MHz. It is based on the digital LLRF system of ALBA [10.3, 10.4], implemented with the RF frequency of MAX IV [10.5] and using commercial uTCA digital boards [10.6, 10.7].

10.6.2 Hardware components

The LLRF hardware will be composed of two main subsystems:

- uTCA chassis + Linux PC + FPGA motherboard;
- front ends.

10.6.2.1 uTCA subsystem

The uTCA subsystem will consist of a uTCA chassis with a minimum of four slots, a uTCA Linux PC, and two uTCA FPGA motherboards plus four FMC boards (see Fig. 10.13).

The main digital processor of this LLRF system will be a Virtex-6 FPGA embedded in a uTCA FPGA motherboard, Perseus, provided by Nutaq. Two FMC boards will be plugged into the first motherboard: one with fast ADCs (MI125) and the other with fast DACs (MO1000). A second uTCA FPGA motherboard and FMC board with fast ADCS (MI125) will be added for extra diagnostics and fast interlock ability. The capabilities of this subsystem are:

- 32 digital inputs;
- 32 digital outputs;
- 2 × FMC MI125 with 16 ADCs—14 bits, 125 MHz, AC coupled, 50 Ω, 10 dBm maximum input;
- FMC MO1000 with 8 DACs—16 bits, 1 GHz, AC coupled, 50 Ω, 10 dBm maximum output;

- 2 × 4 slow ADCs—12 bits, 250 kHz;
- external and internal clocks;
- 2 × 1 GB RAM for post-mortem analysis.

10.6.2.2 Front end

The front end will be used to distribute the RF signals to the digital boards of the LLRF, and it will up-convert the control signals provided by the digital boards from intermediate frequency (IF) to RF. It will also contain pin diode switches to cut the LLRF drives in case an interlock is detected.

In addition, the front end would provide access to the BNC test point to connect the RF signals being analysed to scopes for diagnostic purposes.

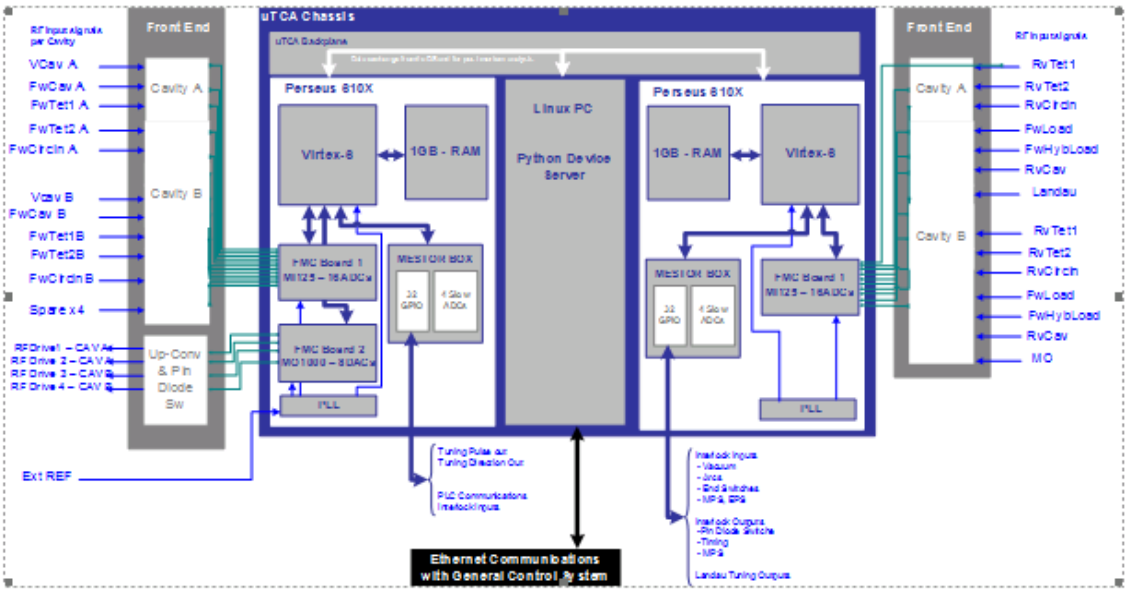

Fig. 10.13: LLRF hardware scheme and signal distribution [10.1]

Figure 10.13 shows the distribution of the signals between the front ends and the digital subsystem, together with the main components of the uTCA system.

A digital patch panel will also be included to adapt the level/logic of digital signals between the LLRF and other systems of the RF plants (motor controllers, programmable logic controllers, machine-protection-system (MPS), etc.).

10.6.3 LLRF firmware description

The main digital signal processing implemented in the FPGA would have the following functionalities:

- monitoring status of RF signals
- controlling amplitude and phase via IQ loops of the cavity field;
- cavity tuning;
- automatic start-up of the system;
- automatic conditioning of the cavity;
- recording of main digital processing signals for post-mortem analysis;
- fast interlock handling.

Figure 10.14 shows a schematic of the main digital signal processing to be applied to the RF signals of each plant.

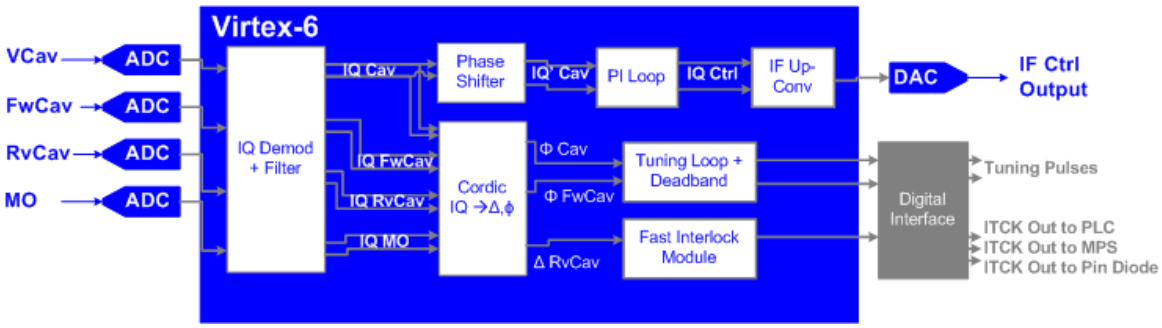

Fig. 10.14: Firmware scheme per RF plant

10.6.3.1 IQ digital demodulation

The RF input signals of the LLRF will be digitalized and IQ demodulated, acquiring 0.75 samples per RF period, as shown in Fig. 10.15. A software counter controlled by the phase of the master oscillator will be used to calculate the relative phase of each signal respect to the MO.

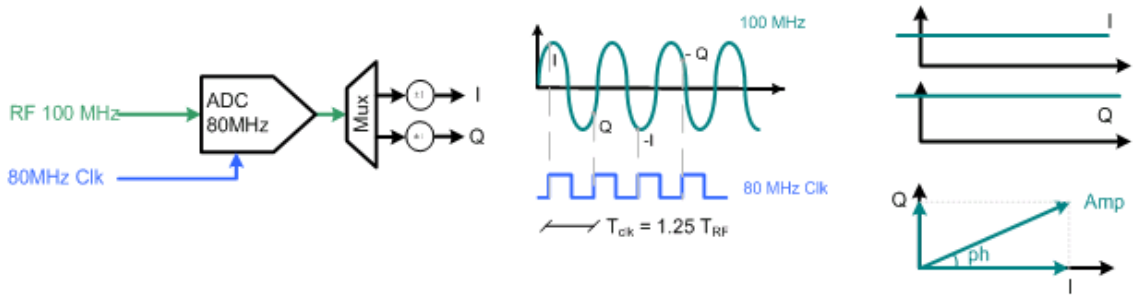

Fig. 10.15: Digital IQ demodulation

10.6.3.2 Control loop specifications

The specifications for the control loops are summarized in Table 10.5.

Table 10.5: Control loop specifications

Loop	Resolution (r.m.s.)	Bandwidth	Dynamic range
Amplitude loop	< 0.5%	⩾ 10 kHz	30 dB
Phase loop	< 0.5°	⩾ 10 kHz	360°
Tuning	< ±1°	—	< ±75°

10.6.3.3 Amplitude and phase loops

When the IQ loops are enabled, the amplitude and phase of the cavity voltage are regulated by controlling the I and Q components of that signal through standard PI loops, as shown in Fig. 10.16. The reference point and parameters of the loop can be adjusted through the graphical user interface (GUI) to make the response of the loop faster or slower (via the constant of proportionality K_p and the integral constant K_i).

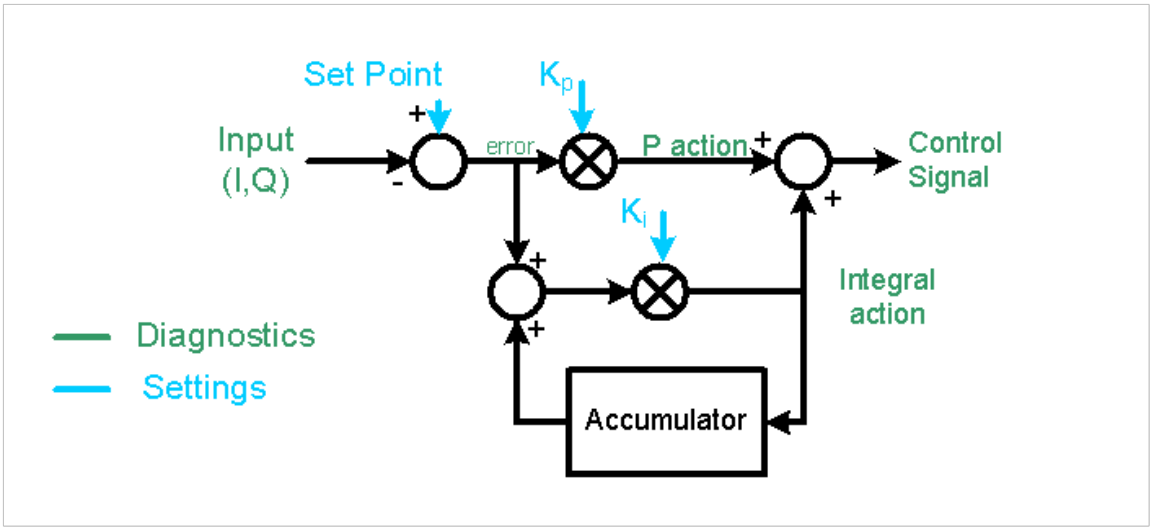

Fig. 10.16: PI loop

When the polar loop mode is enabled, the user can directly control the amplitude independently of the phase. It is also possible to control either the amplitude of one signal (e.g. the cavity voltage) or the phase of another signal (e.g. the forward power of the cavity). This would allow the user to set different bandwidths for the loops.

The amplitude loop bandwidth can work between sub-Hz to a few kHz, while the phase loop can work with a minimum bandwidth of 1–50 kHz.

10.6.3.4 Tuning loop

The tuning loop of the cavities measures the phase difference between the cavity voltage and the forward cavity voltage. If this phase difference is out by a certain margin, which is adjustable by the user, the board sends a train of pulses to move a stepper motor in order to change the shape of the cavity and adjust its resonance frequency.

The cardiac algorithm will be used to translate IQ coordinates to polar coordinates and to compute the tuning diphase. The digital interface will adapt the FPGA digital outputs to the levels required by the motor controller of the cavities plunger. An external parameter will also allow the user to select the frequency of the pulses (from a few Hz to kHz).

10.6.4 LLRF extra utilities

A series of extra utilities will be implemented in the digital LLRF to improve the operability of the RF system. Some examples are listed.

- **Ramping:** A special operation mode could be implemented to ramp the RF power, whereby the voltage of the cavity would be increased following a ramp after a trigger is received. The parameters will be adjustable by the user.
- **Fast interlock:** The reverse power of the cavity will be monitored by the LLRF, and in case its amplitude exceeds a certain value defined by the user, a digital output will be sent from the FPGA board to the digital board interface. The digital interface will then pass this signal on to a fan out so the fast interlock can be transferred to the relevant subsystems to stop the RF plant redundantly.
- **Automatic start-up:** The automatic start-up procedure would allow the user to set a plant in operation after an interlock or a shutdown by following a series of steps, and it will inform the user when the system is ready to operate with beam. This utility has been developed for better usability and fast recovery of the system.

- **Automatic cavity conditioning:** In order to make the conditioning of the cavities easier, a special mode will be implemented in the LLRF whereby the RF drive output will be pulse modulated. The user would be able to set the voltage to be achieved by the cavity, and the system will automatically increase the power to the cavity upon checking the vacuum information.
- **Fast data logger for post-mortem analysis:** The 1 GB RAM would be used to store different diagnostic signals involved in the main digital signal processing of the board, which could be retrieved after interlock detection for post-mortem analysis or upon request by the user. Up to 420 ms of operation data from the two RF plants could be stored simultaneously in the 1 GB RAM of the Perseus system.

References

[10.1] Å. Andersson *et al*., The 100 MHz RF system for the MAX IV storage rings, Proc. IPAC2011, San Sebastián, Spain, 4–9 September 2011, p. 193. https://inspirehep.net/record/1183697

[10.2] P.F. Tavares *et al*., *Phys. Rev. Spec. Top. Accel. Beams* **17** (2014) 1, https://doi.org/10.1103/PhysRevSTAB.17.064401

[10.3] A. Salom and F. Pérez, Digital LLRF for ALBA storage ring, Proc. EPAC2008, Genoa, Italy, 23–27 June 2008, p. 1419. https://inspirehep.net/record/794824

[10.4] A. Salom, B. Bravo, J. Marcos, and F. Perez, ALBA LLRF upgrades to improve beam availability, Proc. IPAC2015, Richmond, Virginia, USA, 3–8 May 2015, p. 1022. https://doi.org/10.18429/JACoW-IPAC2015-MOPTY042

[10.5] A. Salom, F. Perez, Å. Andersson, R. Lindvall, L. Malmgren, A.M. Milan, and A.M. Mitrovic, Digital LLRF for MAX IV, Proc. IPAC2017, Copenhagen, Denmark, 14–19 May 2017, p. 4037, https://doi.org/10.18429/JACoW-IPAC2017-THPAB135

[10.6] A. Salom, E. Morales, and F. Perez, Development of a DLLRF using vommercial uTCA platform, Proc. IPAC2017, Copenhagen, Denmark, 14–19 May 2017, p. 3631. https://doi.org/10.18429/JACoW-IPAC2017-THOAA1

[10.7] Nutaq, https://web.archive.org/web/20181204123128/https://www.nutaq.com/, last accessed December 4th 2018.